Smart Structures and Systems, *Vol. 14, No. 3 (2014) 347-365*
DOI: http://dx.doi.org/10.12989/sss.2014.14.3.347

Positioning and vibration suppression for multiple degrees of freedom flexible structure by genetic algorithm and input shaping

J. Lin* and C.B. Chiang

Department of Mechanical Engineering, Chien Hsin University of Science and Technology
229, Chien-Hsin Rd., Jung-Li City, Taiwan 320, R.O.C.

(Received January 22, 2013, Revised July 15, 2013, Accepted August 1, 2013)

Abstract. The main objective of this paper is to develop an innovative methodology for the vibration suppression control of the multiple degrees-of-freedom (MDOF) flexible structure. The proposed structure represented in this research as a clamped-free-free-free truss type plate is rotated by motors. The controller has two loops for tracking and vibration suppression. In addition to stabilizing the actual system, the proposed feedback control is based on a genetic algorithm (GA) to seek the primary optimal control gain for tracking and stabilization purposes. Moreover, input shaping is introduced for the control scheme that limits motion-induced elastic vibration by shaping the reference command. Experimental results are presented, demonstrating that, in the control loop, roll and yaw angles track control and elastic mode stabilization. It was also demonstrated that combining the input shaper with the proportional-integral-derivative (PID) feedback method has been shown to yield improved performance in controlling the flexible structure system. The broad range of problems discussed in this research is valuable in civil, mechanical, and aerospace engineering for flexible structures with MDOM motion.

Keywords: large flexible structures; genetic algorithms; input shaping; multiple degrees of freedom; vibration suppression

1. Introduction

A great deal of interest exists in finding control methods that will eliminate vibration from a wide variety of mechanical and structural systems. Among these, smart structures have attracted significant attention to date from researchers in the field of dynamics and control. The control of flexible structures has drawn much attention recently and will continue to be a vigorous area of research as all machines exhibit flexibility while being pushed to their performance limits (Hyland *et al*. 1993).

The broad usage of large flexible structures (LFS), coupled with the need to control unwanted vibrations, has motivated a large amount of research pertaining to the control of these structures. However, problems have arisen, especially concerning the control of flexible robots (Lin and Lewis 2003, Rhim and Book 2001), smart panels (Lin 2005a, Lin 2005b, Qiu *et al*. 2007, Lin and

*Corresponding author, Professor, E-mail: jlin@uch.edu.tw

http://www.techno-press.org/?journal=sss&subpage=8 ISSN: 1738-1584 (Print), 1738-1991 (Online)

Zheng 2012, Li *et al*. 2011), aircraft fin-tip (Hu 2008, Rao *et al*. 2008), satellites, and space stations that have solar array paddles (Matsuno *et al*. 1996). Researchers have sought to improve the positioning capability and eliminate the motion-induced oscillation. The control strategies proposed to suppress these induced elastic modes for LFS include combining positive position feedback (PPF) and proportional-derivative (PD) control (Qiu *et al*. 2007), robust H_∞ controller (Rao *et al*. 2008), output feedback, and state feedback (Hong *et al*. 2006) as well as using a robust suppression controller (Fujisaki *et al*. 2001, Nagashio and Kida 2009). However, previous research has displayed only numerical simulation results; no experimental verification has been presented.

In addition, input shaping is a common filtering method for reducing motion-induced vibration wherein the reference command is altered by convolving it with a series of impulses (Blackburn *et al*. 2010). Such a control scheme is implemented by convolving a sequence of impulses, known as an input shaper, with a baseline command. The input shaper is designed using rough estimates of system natural frequencies and the damping ratio. Instead of the original baseline command, the convolution product is then issued to the plant (Sorensen and Singhose 2008). In the past few decades, input shaping has been shown to be very effective on flexible manipulators (Rhim and Book 2001), spacecraft (Hu 2008), satellites (Tuttle and Seering 1996), and bridge cranes (Blackburn *et al*. 2010, Khalid *et al*. 2006, Singhose *et al*. 2008, Sorensen *et al*. 2007, Vaughan *et al*. 2010), even when the payload undergoes moderate hoisting. Most input-shaping techniques are based upon the linear system theory. However, some researchers' efforts have examined the extension of input shaping to the nonlinear system. Modified input shaping methodologies presented by some researchers have included the command shaping technique and positive position feedback control (Hu 2008), nonlinear input shaping (Park and Chang 2001), a robust input shaper (Vaughan *et al*. 2008), and an adaptive or learning input shaper (Cutforth and Pao 2003, Cutforth and Pao 2004). However, such studies deal only with the fixed flexible structures and have not looked considerably into trajectory tracking.

It is well known that the input shaper is an open-loop controller, which has the limitation of dealing with parameter changes and disturbances to the system. Moreover, this technique requires relatively precise and dynamic knowledge of the system, even if several designs have been proposed to improve the robustness of input shaping to the damping factors and natural frequencies of the flexible structures (Hu 2008, Vaughan *et al*. 2008, Cutforth and Pao 2003, Cutforth and Pao 2004). It should also be noted that the plant being linear is essential for proving why input shaping techniques work. Thus, how to introduce the input shaping control technology in a nonlinear plant becomes a challenging topic for controller design.

Hence, this work tries to investigate the effect of nonlinear multiple-degree-of-freedom flexible structures on the performance of input shaping. The study demonstrates that, for the multiple-degree-of-freedom (MDOF) rotating plate, nonlinear dynamics can be significant. Novel command-shaping algorithms are then proposed for dealing with the nonlinear MDOF rotating plate. Even if the results of this analysis are developed for a flexible plate, they can also be extended to be useful in civil, mechanical, and aerospace engineering for flexible structures with MDOF motion.

2. Dynamic system description

The proposed MDOF flexible structure model of this research is a clamped-free-free-free (CFFF) truss type plate, as shown in Fig. 1. Assuming that the clamped-free-free-free truss plate is

clamped on a rigid frame along the $\mathbf{Z}_0$ axis, the instantaneous transverse elastic displacement along the $\mathbf{Y}_0$ axis is $w(x, z, t)$. The truss type plate is rotated by motor 1 about the $\mathbf{Y}_0$ axis (roll axis). It is also rotated by motor 2 about the central axis $\mathbf{Z}_0$ (yaw axis) of the plate. For the convenience of the analysis, assume that w is separable into its temporal and spatial components.

Accordingly, the classical differential equation of motion for the transverse displacement w of a plate is given by (Leissa 1969)

$$D\nabla^4 w + \rho \frac{\partial^2 w}{\partial t^2} = 0 \tag{1}$$

The plate has a thickness h, a mass per unit area ρ, Poisson's ratio ν, and Young's modulus E; t is the time, and $\nabla^4 = \nabla^2\nabla^2$. Thus, the flexural rigidity is defined as

$$D = h^3 E / 12(1-\nu^2) \tag{2}$$

When free vibrations are assumed, the motion is expressed as

$$w = W \cos \omega t \tag{3}$$

where ω is the circular frequency, and W is a function of only the position coordinates. The boundary conditions for CFFF plate are (Lin and Zheng 2012)

$$\begin{aligned} &w = 0, \frac{\partial w}{\partial x} = 0, M_{xz} = 0 \quad (x = 0) \\ &M_x = 0, S_x = 0, M_{xz} = 0 \quad (x = a) \\ &M_z = 0, S_z = 0, M_{zx} = -M_{\mathbf{xz}} = 0 \ (z = \pm b) \end{aligned} \tag{4}$$

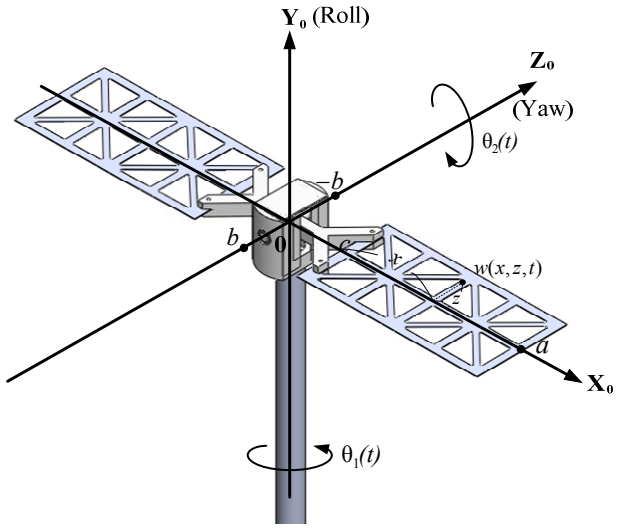

Fig. 1 Conceptual model of the MDOM flexible structure system

where M_x, M_z, and M_{zx} are the internal moments along *x*, *z* axis, and *xz* plane, respectively. Moreover, S_x and S_z are the shear forces along *x*, *z* axis, respectively.

As the plate has a CFFF boundary condition, the mode shape functions are given by

$$W(x,z)=\sum_{i=1}^{m}\left\{A_{i1}+A_{i2}\sqrt{3}\left(1-2\frac{z}{a}\right)+\sum_{j=3}^{n}A_{ij}\left[\cosh\frac{\varepsilon_j z}{2b}+\cos\frac{\varepsilon_j z}{2b}-\alpha_j(\sin\frac{\varepsilon_j z}{2b}+\sin\frac{\varepsilon_j z}{2b})\right]\right\} \tag{5}$$

$$\times\left[\cosh\frac{\varepsilon_i x}{a}-\cos\frac{\varepsilon_i x}{a}-\alpha_i(\sin\frac{\varepsilon_i x}{a}+\sin\frac{\varepsilon_i x}{a})\right].$$

where the values of *m* and *n* are truncated modes for *x* and *z* direction, respectively, and A_{ij}, α, and ε are the parameters of the mode shape function (Leissa 1969). The detailed values for A_{ij}, α, and ε can be also refer to Leissa (1969).

Let θ_i, J_i, u_i, and g_{r_i} (*i*=1,2) be, respectively, the rotation angle, the moment of inertia of the rotor, the driving torque, and the gear ratio of motor *i*. The total kinetic energy *K* is given by

$$\begin{aligned}K=&\frac{1}{2}J_1g_{r1}^2\dot{\theta}_1^2+\frac{1}{2}J_2g_{r2}^2\dot{\theta}_2^2\\&+\frac{1}{2}\rho\int_{-b}^{b}\int_0^a[(y\dot{\theta}_2+\dot{w})^2+(c+x)^2\dot{\theta}_1-2(c+x)\dot{\theta}_1(y\dot{\theta}_2+\dot{w})\cos\theta_2]dxdz\end{aligned} \tag{6}$$

Moreover, it is often useful to know the strain energy stored in a plate due to deformation. One such instance occurs when the Rayleigh-Ritz method is applied in order to obtain approximate solutions. For an isotropic plate, the strain energy due to bending becomes (Leissa 1969)

$$P=\frac{1}{2}D\int_{-b}^{b}\int_0^a\left\{\left(\frac{\partial^2 w}{\partial x^2}+\frac{\partial^2 w}{\partial z^2}\right)-2(1-\nu)\left[\frac{\partial^2 w}{\partial x^2}\frac{\partial^2 w}{\partial z^2}-\left(\frac{\partial^2 w}{\partial x\partial z}\right)^2\right]\right\}dxdz \tag{7}$$

Nevertheless, the potential energy owing to gravity can be cancelled by a strain-energy term that is caused by the fact that the strain-energy stored in an elastic element is a function of how much it is deflected from its free length, rather than the static-equilibrium position from which the vibration amplitude is computed. Hence, the potential energy due to gravitation can be ignored in this research.

By using the Lagrangian formulation—and after some complicated calculations—the equation of vibration of the flexible plate can be referred to (Lin and Zheng 2012, Matsuno *et al*. 1996) and summarized as follows

$$\ddot{w}+\frac{EI}{\rho}(\frac{\partial^4 w}{\partial x^4}+2\frac{\partial^4 w}{\partial x^2\partial z^2}+\frac{\partial^4 w}{\partial z^4})=(c+x)\cos\theta_2\ddot{\theta}_1(t)-z\ddot{\theta}_2(t) \tag{8}$$

and the equations of the angles of rotation of motors 1 and 2 are

$$\begin{aligned}&\Gamma(\theta_2)\ddot{\theta}_1(t)+\frac{\cos\theta_2}{g_{r1}}\left(c\int_{-b}^{b}Q_x\big|_{x=0}dz-\int_{-b}^{b}M_x\big|_{x=0}dz\right)=u_1(t)\\&J_2g_{r2}\ddot{\theta}_2(t)-\frac{1}{g_{r2}}\left(\int_{-b}^{b}Q_x\big|_{x=0}dz\right)=u_2(t)\end{aligned} \tag{9}$$

where Q_x is the shearing force acting on the edges aligned along the *x* axis and

$\Gamma(\theta_2) = J_1 g_{r1} + \frac{\rho}{g_{r1}} \int_{-b}^{b} \int_{0}^{a} x^2 \sin^2\theta_2 dxdz$.

In order to simplify the implementation of the control algorithm, this research introduces a reduced-order modeling strategy to decompose the complex system into a slow (joint angle) and fast (vibration) subsystem (Lin and Lewis 2003). Thus, by defining the state vector $\mathbf{x} = \begin{bmatrix} \theta_1 & \theta_2 & \dot{\theta}_1 & \dot{\theta}_2 \end{bmatrix}^{\mathbf{T}}$ and servomotors control input $\mathbf{u} = \begin{bmatrix} u_1 & u_2 \end{bmatrix}^T$, the system for (9) can be described as

$$\dot{\mathbf{x}} = f(\mathbf{x}, \mathbf{u}), \quad \mathbf{x}(0) = \mathbf{x_0} \tag{10}$$

where $\mathbf{x}(0)$ is the initial condition of the state vector.

Using the nominal (equilibrium) point $\mathbf{x}^*$, the approximated linear model for the system can be rewritten as

$$\begin{aligned} \dot{\mathbf{x}} &= \mathbf{A}\mathbf{x} + \mathbf{B}\mathbf{u} \\ \mathbf{y} &= \mathbf{C}\mathbf{x} \end{aligned} \tag{11}$$

where $\mathbf{A} = \left(\frac{\partial f(\mathbf{x},\mathbf{u})}{\partial \mathbf{x}}\right)_{(\mathbf{x}=\mathbf{x}^*)}$, $\mathbf{B} = \left(\frac{\partial f(\mathbf{x},\mathbf{u})}{\partial \mathbf{u}}\right)_{(\mathbf{x}=\mathbf{x}^*)}$.

It is worth noting that the above Eq. (11), which includes some vibration information, dominates the joint angle trajectory tracking.

3. Controller design

The control objective is to determine the input control torque, u, so that the transverse elastic displacement of plate *w* damps out as efficiently as possible while the joint angles $\theta_i(t)$ (*i*=1, 2) follow the desired track $\theta_{id}(t)$. Let $\theta_{id}(t)$ be the desired trajectory that each motor angle $\theta_i(t)$ should follow and define

$$e_{\theta_i} = \theta_i - \theta_{id} \tag{12}$$

$$\dot{e}_{\theta_i} = \dot{\theta}_i - \dot{\theta}_{id} \tag{13}$$

For such case, the joint angles tracking control is defined as roll and yaw angles track. The controller developed for this research will be combined with positioning and oscillation suppression properties by merging PID feedback control with input shaping. The control is comprised of two modules that have been combined into unified control architecture. A feedback control module based on genetic algorithm (GA) tuning is used to drive the plate to the desired position. Input shaping is used in another module to eliminate motion-induced vibration. A block diagram of the overall control system is demonstrated in Fig. 2. The methodology by which the combined control accomplishes the control objectives is easily understood by separately considering the individual modules comprising the controller. The following subsections provide a

description of the two modules.

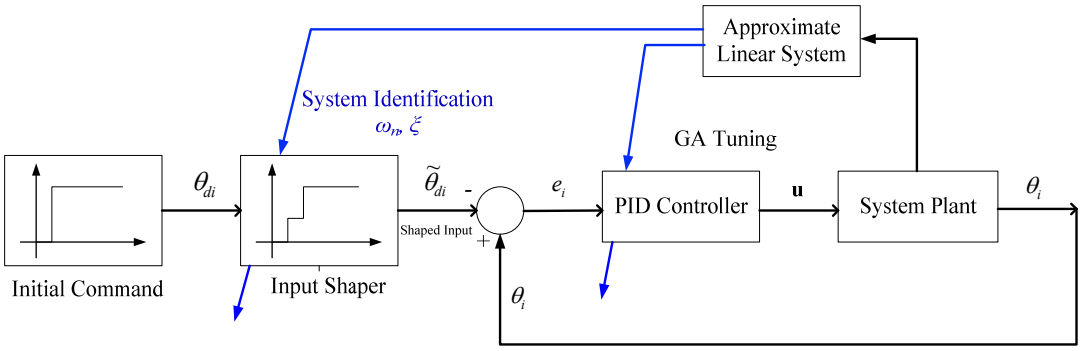

Fig. 2 Block diagram of the overall control system

3.1 Find the near-optimum feedback controller

The main objective of such a design is to improve the controllability of the overall system. In practice, deriving exact mathematical models for such complicated structure is extremely difficult. The detailed model derived in Section 2 is useful for modal analysis, particularly for a system setup. However, the derived model is quite complicated and the resulting controller order might be too high to be implemented with a satisfactory performance. However, for an unstable nonlinear model, a nonlinear model can be linearized and the linear model stabilized by using linear control schemes (Lin and Zheng 2012). Hence, the proportional-integral-derivative (PID) controller can serve as an assistant controller to stabilize the linear system. Thus, the first task of such a control algorithm is to find a near-optimum PID controller. Let us introduce the approximately second-order linear control system from (11), which includes some vibration information

$$\mathbf{G}_{CL}(s) = \mathbf{C}(s\mathbf{I} - \mathbf{A})^{-1}\mathbf{B} \tag{14}$$

In some cases, **A**, **B**, and **C** are not known exactly. As such, $\hat{\mathbf{A}}$, $\hat{\mathbf{B}}$, and $\hat{\mathbf{C}}$ could be the best estimate we have for these terms. For such cases, Eq. (14) can be rewritten as

$$\mathbf{G}_{CL}(s) = \hat{\mathbf{C}}(s\mathbf{I} - \hat{\mathbf{A}})^{-1}\hat{\mathbf{B}} \tag{15}$$

In fact, even if the matrix consists of $\hat{\mathbf{A}} \neq \mathbf{A}$, $\hat{\mathbf{B}} \neq \mathbf{B}$, and $\hat{\mathbf{C}} \neq \mathbf{C}$, the performance of controllers based on Eqs. (14) and (15) can be quite good if the outer-loop gains are appropriately selected (Lin and Zheng 2012).

Moreover, the PID standard form is

$$\mathbf{u} = -\mathbf{K}_\mathbf{P}\mathbf{e} - \frac{\mathbf{K}_\mathbf{I}}{s}\mathbf{e} - \mathbf{K}_\mathbf{D}s\mathbf{e} \tag{16}$$

where **e** is the tracking error signal, **u** the control action, $\mathrm{K_P}$, $\mathrm{K_I}$, and $\mathrm{K_D}$ are the proportional, integral, and derivative gain, respectively.

Therefore, in order to find the near-optimum feedback controller, the parameters of PID control, based on GA will be introduced. The GA uses the coding of the parameter set to find the concentration of the near optimum points. It was suggested that the optimization problem for picking the control parameters could be constructed as

$$\min \left\| \mathbf{G}_{CL}(j\omega) \right\| \tag{17}$$

where the H_∞-norm of the closed-loop transfer function is to be minimized (Moheimani *et al*. 2006). The fundamental working principle for the proposed GA PD control can refer to (Lin and Zheng 2012). However, the PID control gains from the GA of this research use only a roughly dynamic model as a positioning control module. In addition, the input shaping control schemes contribute to the improvement of the vibration suppression.

3.2 Fundamentals of input shaping

Assuming that a linear second-order system is demonstrated as

$$G(s) = \frac{\omega_n^2}{s^2 + 2\xi\omega_n s + \omega_n^2} \tag{18}$$

with natural frequency ω_n and damping ratio ξ, then for system (18), the response to a sequence of $\overline{N}$ impulses is described as

$$\mathrm{Y} = \exp(-\xi\omega_n t_{\overline{N}})\sqrt{\mathbf{C}^2 + \mathbf{S}^2} \tag{19}$$

where

$$\begin{aligned} \mathbf{C} &= \sum_{i=1}^{\overline{N}} A_i e^{\xi\omega_n t_i} \cos(\omega_d t_i) \\ \mathbf{S} &= \sum_{i=1}^{\overline{N}} A_i e^{\xi\omega_n t_i} \cos(\omega_d t_i) \end{aligned} \tag{20}$$

where A_i and t_i are the amplitude and the application time of the *i*-th impulses, respectively, and $\omega_d = \omega_n\sqrt{1-\xi^2}$ is the corresponding damped natural frequency.

Thus, Eq. (19) represents the percentage residual vibration induced by an impulse sequence given any value of frequency and any damping ration less than 1. A constraint on residual vibration amplitude can be formed by setting Eq. (18) less than or equal to a tolerable level of residual vibration at any desired frequency and damping ratio. If the actual structural frequencies coincide with the concept for designing the shaper, then the oscillation will be attenuated. Specifically, if a series of impulses are to produce zero residual vibration, then the resulting series of impulses is called the Zero Vibration Shaper (ZVS) (Sorensen *et al*. 2007, Park and Chang 2001). Consequently, the parameters to be determined for the ZVS technique design use the following constraints:

$$\sum_{i=1}^{\overline{N}} A_i e^{\xi\omega_n t_i} \cos(\omega_d t_i) = 0$$
$$\sum_{i=1}^{\overline{N}} A_i e^{\xi\omega_n t_i} \sin(\omega_d t_i) = 0 \tag{21}$$

Due to the transcendental nature of the residual oscillation Eq. (21), there are an infinite number of solutions. Moreover, to guarantee that the system reaches the desired state, impulse amplitudes are constrained to be positive and are also constrained to sum to one

$$\sum_{i=1}^{\overline{N}} A_i = 1; \quad A_i > 0, \quad i = 1,2,3....,\overline{N} \tag{22}$$

However, even with such constraints there are still an infinite number of solutions. Hence, to ensure the shortest duration shaper solution, the final necessary design constraint minimizes the time of the final input shaper impulse (Sorensen *et al*. 2007, Park and Chang 2001)

$$\min(t_i) \tag{23}$$

The goal of the current study is to introduce ZVS, which contains two impulses (*i*=2), to yield zero residual vibration. To minimize the time delay, the first impulse must be placed at time zero $t_1 = 0$. Hence, Eq. (21) becomes

$$A_1 + A_2 e^{\xi\omega_n t_2} \cos(\omega_d t_2) = 0 \tag{24}$$

$$A_2 e^{\xi\omega_n t_2} \sin(\omega_d t_2) = 0 \tag{25}$$

$$A_1 + A_2 = 1 \tag{26}$$

where A_1 and A_2 are the impulse amplitudes that occur at time t_1 and t_2, respectively.

To satisfy (25) and keep the impulse sequence as short as possible, the argument of the sine term must equal zero ($A_2 \neq 0$). From this understanding, we get

$$\sin(\omega_d t_2) = 0; \quad \omega_d t_2 = \pi$$
$$\Rightarrow t_2 = \frac{\pi}{\omega_d} = \frac{T_d}{2}; \tag{27}$$

where t_2 is the period of oscillation being suppressed.

In other words, the second impulse must occur at the one-half period of the damped natural frequency. Substituting (27) into (24) and utilizing (26), it can then obtain a closed-form solution

$$A_1 = \frac{1}{1+K_s}$$
$$A_2 = 1 - \frac{1}{1+K_s} \tag{28}$$

where $K_s = exp(\frac{-\xi\pi}{\sqrt{1-\xi^2}})$.

Consequently, the ZVS is given by

$$\begin{bmatrix} A_i \\ t_i \end{bmatrix} = \begin{bmatrix} \frac{1}{1+K_s} & \frac{K_s}{1+K_s} \\ 0 & 0.5T_d \end{bmatrix} \tag{29}$$

The two-impulse sequence given by (27)-(29) is called a ZVS because it satisfies the constraint that the residual vibration must be zero while the model is perfect.

3.3 System identification of modal frequencies and the damping ratio of the system

Estimates of the modal frequency and damping are used to design the timings and amplitudes of the shaper's impulses so that the residual vibration is eliminated or reduced after the end of the shaped command. However, the modeled frequency or damping is often not accurate in systems due to uncertainties. Thus, this study adopts the MATLAB System Identification toolbox to approximate the modal frequency and damping ratio for the input shaper design of the structural system. A model of the structure, which relates input signals to system outputs, is needed for system identification. Thus, a series of input-output pair data based on the experiment needs to be constructed to appropriately describe the system. To improve the accuracy of the system description, a model based on the first experiment is conducted for the second identification experiment. MATLAB's System Identification toolbox allows for an approximated model to be adopted. However, the calculation of the modal natural frequencies and damping ratios through the system identification scheme are not all are applicable for the controller design. This study introduces input shaping for the control scheme to limit the motion-induced elastic vibration by shaping the reference command. Hence, to guarantee that the system reaches the desired state, impulse amplitudes are constrained to be positive and are also constrained to sum to one. In addition, to ensure the shortest duration of the shaper solution, the final necessary design constraint minimizes the time of the final input shaper impulse.

4. Experimental verification

To assess the merit of the proposed control concepts, a number of experiments were carried out using such a structure, using an accelerometer to detect local vibrations. The configuration of the test-bed is similar to reference (Lin and Zheng 2012). The main structure of this proposed system basically includes a base, support mast, connecting rod, two truss type plates, and two drive units. The geometric size and two-axis motion of the proposed system is demonstrated in Fig. 3. The first drive servomotor connects the mast and leads the mast rod rotation. Moreover, the crossbar located at the top of the mast acts as a transverse axis. The second servomotor is spindled with the crossbar using a steel-rope drive. Thus, the second drive unit links to the cross rod and leads the cross rod to turn in a yawing motion. As a result, the driving motions to the mast and the cross rod yield the roll and yaw axis motion. The complete system is installed in the Sensor and Control Laboratory at the Department of Mechanical Engineering, Chien Hsin University of Science and Technology

(Fig. 4). The controller was implemented using MATLAB and Simulink during experiments. Although the test-bed of this study is similar to reference (Lin and Zheng 2012), this study made some improvements in mechanism design to reduce noise and friction disturbances during the motion. The comparison of the mechanism design between reference (Lin and Zheng 2012) and the current test-bed is indicated in Fig. 5. The detailed mechanism improvement results are demonstrated in (Chiang 2012).

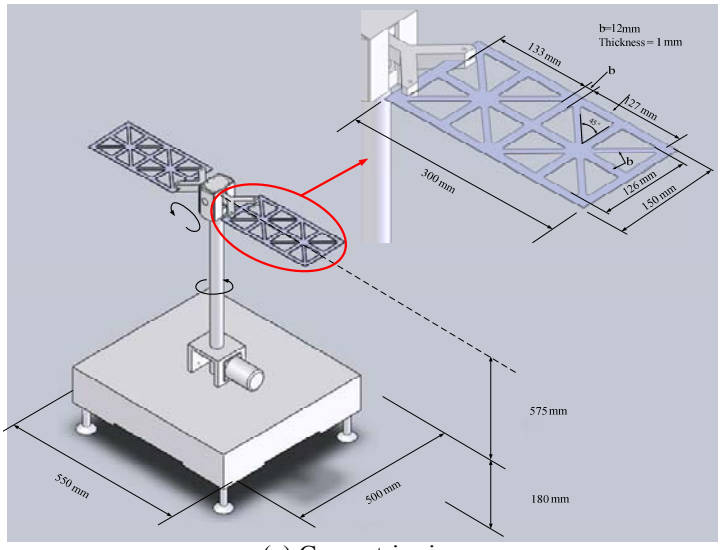

(a) Geometric size

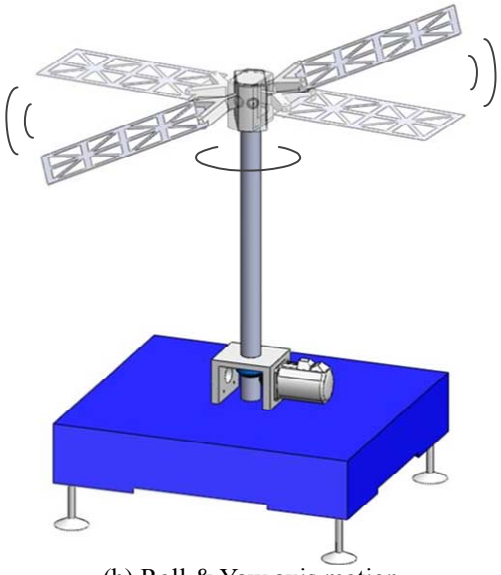

(b) Roll & Yaw axis motion

Fig. 3 Motion of the proposed system

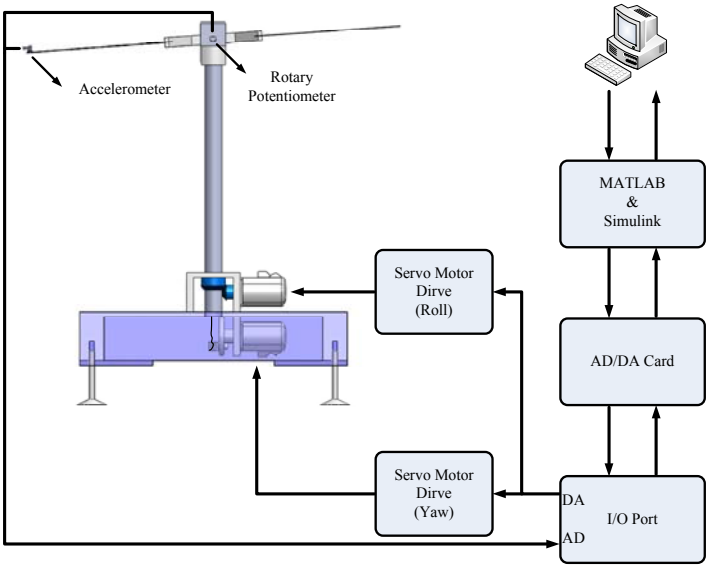

Fig. 4 Implementation of the control structure

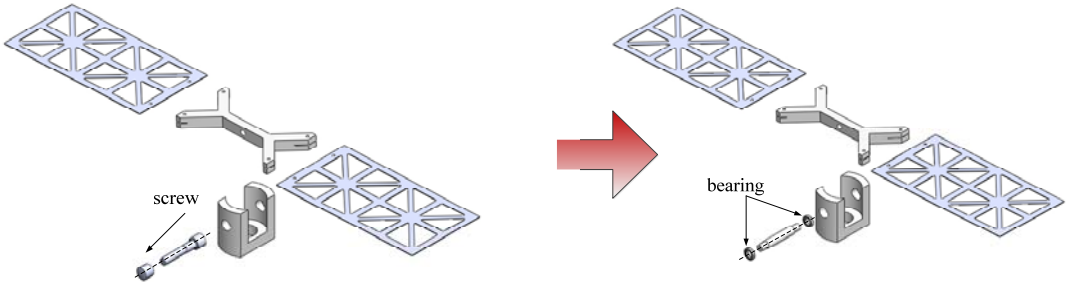

(a) Truss plate

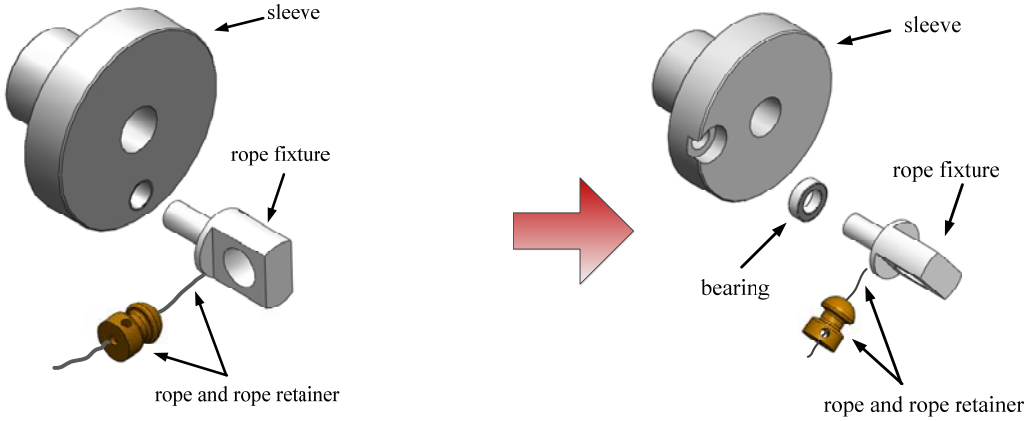

(b) Steel-rope drive unit

Fig. 5 Improvement in the mechanism design: this study (right) and reference (Lin and Zheng 2012) (left)

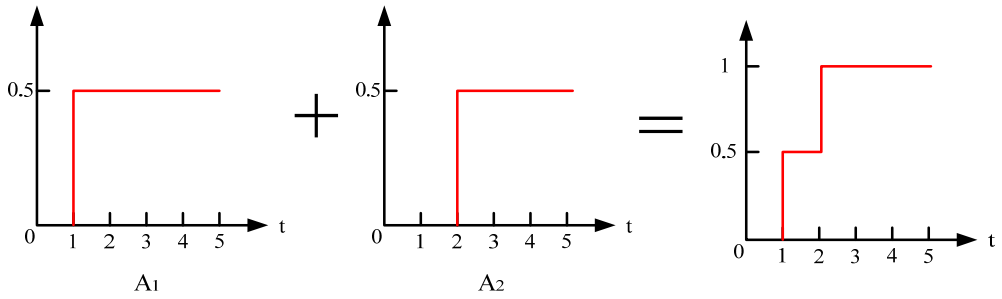

Fig. 6 Principles of Step Superposition (SS)

This section presents experimental results for the application of the proposed controller. In this vibration control problem, vibrational displacement of the rotating plate is markedly affected by the axis motion. The controller developed for this research was combined with positioning and vibration suppression modules. The positioning control module enabled the plate to achieve the desired position as well as slightly reduce the motion-induced vibration as the controller design was based on the approximated linear system, which included some vibration information that dominated the joint angle trajectory tracking. A more desirable input shaping control scheme allowed for the elimination of these motion-induced vibrations in-depth. In this experiment, we considered a two-axis motion (roll and yaw motion) for such a structure. To stabilize the actual system, the proposed GA PID control must supplement an input shaping law to ensure a stable nonlinear system. Therefore, a controller based on input shaping incorporated with feedback control based upon GA tuning was used to increase the efficiency of control. In addition, two input shaping methodologies—step superposition (SS) and zero vibration shaper (ZVS)—were implemented for control purposes. Comparisons were made between SS and ZVS. The SS is defined an equal length shaped input as demonstrated in Fig. 6.

In order to determine the location with the greatest vibration amplitude, the rotating plate was divided into 7 points (Fig. 7). In the open-loop control, the fast Fourier Transform (FFT) analysis verified that the maximum magnitude of the vibration amplitude is located at points 2 and 3 subjected to input commands (Lin and Zheng 2012). Hence, the following experimental results will present only the test data at points 2 and 3.

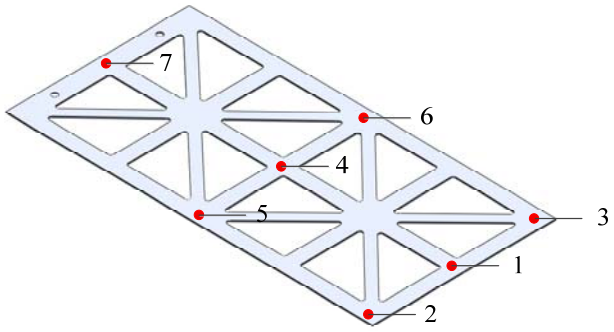

Fig. 7 Vibration sensing point for rotating plate

Because the vibration is eliminated only after the end of the shaped input command, making the input shaper length as short as possible is desirable to ensure that shaping does not significantly increase the maneuver time. Thus, in order to design an input shaper so that residual vibration in the system output is reduced, knowledge about the modal natural frequency ω_n and damping ratio ξ is needed.

This section presents experimental results for the application of the proposed controller. In this vibration control problem, vibrational displacement of the rotating plate is markedly affected by the axis motion. The calculation for control results is obtained by the procedures presented in Section 3.

In order to evaluate the performance of the proposed control scheme, the GA model was given a crossover rate of 0.9 and a mutation rate of 0.03 in order to first seek the near-optimum PID controller. The population size was set at 50, and the maximum of the number of generations was set at 30. Thus, the near optimum control gains for the tracking controller were $\mathrm{K_P} = 6$, and $\mathrm{K_D} = 0.5$ for the roll axis. Similarly, the control gains for the yaw axis were $\mathrm{K_P} = 1$, $\mathrm{K_D} = 0.1$, and $\mathrm{K_I} = 0.15$. In order to eliminate signal noise from the accelerator sensor, the filter was designed as a 100-Hz 8th order Butterworth low-pass filter.

Furthermore, to estimate the appropriate modal frequency and damping ratio for designing the ZVS, the system identification approach was introduced. A series of input-output pair data were constructed to appropriately describe the system, and MATLAB's System Identification toolbox allowed for an approximated model. However, the calculation of the natural frequencies and damping ratios through system identification scheme were not all applicable for the controller design. If the range of frequencies and expected damping in a system as well as the lengths of input commands are known, it is possible to weigh the benefits of shaped inputs. Hence, to guarantee that the system reaches the desired state, impulse amplitudes were constrained to be positive and to sum to one. In addition, to ensure the shortest duration shaper solution, the final necessary design constraint minimized the time of the final input shaper impulse. Based on these two concepts, the parameters of the ZVS were designed as $\omega_n = 13$ and $\xi = 0.2$ for roll motion and $\omega_n = 4$ and $\xi = 0.1$ for yaw motion. The original, SS, and ZVS shaped commands for the roll and yaw axis motions are demonstrated in figure 8. The solid line (blue) is the initial input command. The dotted line (orange) is the SS shaped command, and the dashed line (red) represents the ZVS shaped command. The shaped command for ZVS varies with the system's modal parameters, which is a major difference from SS, which is defined as an equal length shaped command.

Combining feed-forward methods (such as input shaping) with feedback method (such as PID) was shown to yield improve performance in the experiment. To verify the controller's performance, step input real-time experiments carried out for the proposed control scheme are described. The desired step inputs were taken as one radian (57.6°) for roll motion and 0.2 radian for yaw motion. Table 1 lists the computation results for the normalized root-mean-square (RMS) tracking error under GA PID control, GA PID combined with SS (indicated as "GA PID + SS" in the table), and GA PID combined with ZVS (indicated as "GA PID + ZVS" in the table). In this study, the comparison joint angle tracking error or vibrational displacement in a normalized root-mean-square (RMS) e_{RMS} is defined as

$$e_{RMS} = \sqrt{\sum_{k=1}^{N} e_k^2} / N \tag{30}$$

where N is total number of samples.

The controlled response verifies that the PID controllers tuned by the GA can effectively track the trajectory of the smart plate. This experimental finding also confirms that the GA PID combined with SS reduces tracking error (RMS) from GA PID by approximately 29.1% for roll motion and 23.2% for yaw motion. Moreover, tracking error can be further reduced by as much as 64% for yaw motion when ZVS is applied. These experimental results demonstrate the effectiveness of the proposed control methodology for minimizing tracking error in the time domain.

Fig. 9 plots the time response of the vibrational displacement under the different control schemes. The GA PID combined with SS achieved better vibration suppression than the GA PID control for point 2 as well as point 3. The equal length shaped input often resulted in less vibration than the original step input command in the time domain.

In addition, the vibration displacement can be further suppressed when the ZVS is applied. Performance was significantly improved for vibrational displacement by adopting the ZVS. As a result, it should be pointed out that the vibration can vary with the length of the command. The vibrational displacement was clearly reduced when feedback loops for tracking and input shaping for damping were applied.

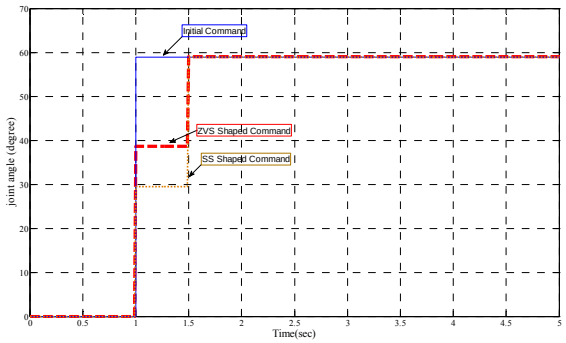

(a) Roll

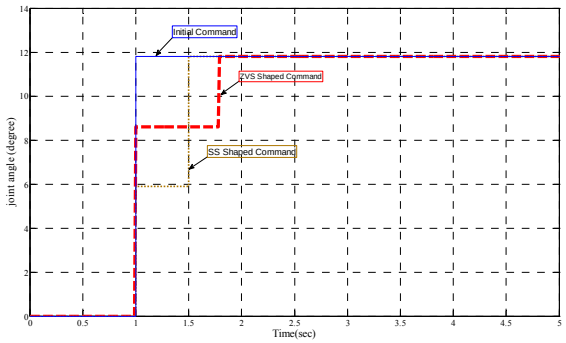

(b)Yaw

Fig. 8 ZVS shaped command for roll and yaw motion

Table 1 Normalized RMS tracking error for different control scheme in roll and yaw motion

Control Type	GA PID	GA PID+SS	GA PID+ZVS
	(A)	**(B)**	**(C)**
Tracking error (Roll) RMS	0.0155	0.011	0.011
Tracking error reduction (%)		(A-B)/A **29.1%**	(A-C)/A **29.1%**
Tracking error (Yaw) (RMS)	0.0125	0.0096	0.0045
Tracking error reduction (%)		(A-B)/A **23.2%**	(A-C)/A **64%**

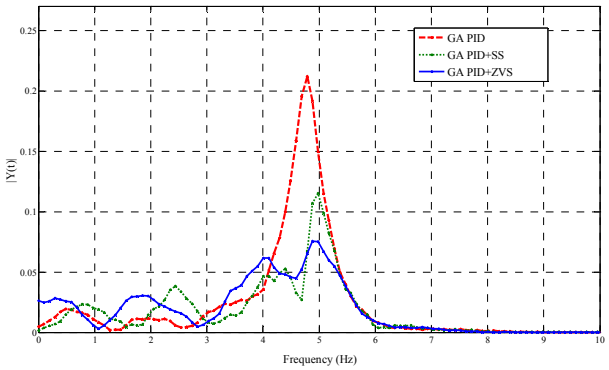

(a)

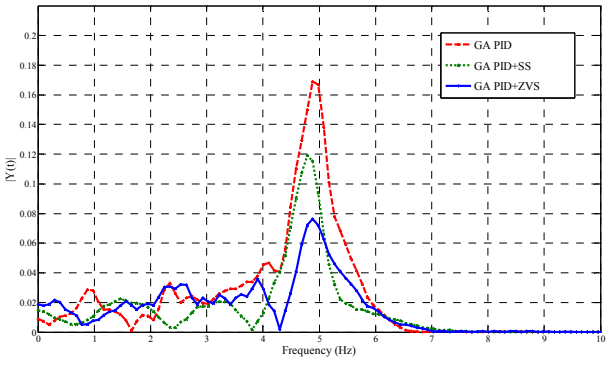

(b)

Fig. 10 Maximum vibration amplitude for different control scheme by FFT analysis (a) Point 2 (b) Point 3

Moreover, the maximum vibration amplitude around the most dominant resonant frequency was significantly reduced, as demonstrated in Fig. 10. As Fig. 10 indicates, a significant amplitude reduction occurs when the SS is applied for point 2 and 3. Furthermore, a greater reduction occurs with the ZVS than with SS. The experiments confirmed the predicted large reduction in the low-mode amplitude when ZVS is utilized. These results are consistent with Table 1. Hence, it can be concluded that the proposed input shaping technique plus feedback control achieves excellent attenuation of vibrations from plate flexing and tracking control.

To further verify the performance of the proposed controller, Tables 2 and 3 compare the normalized root-mean-square (RMS) accelerator output voltage and maximum vibration amplitude around the resonant frequency, subjected to a step command, for different control methodologies. The tables indicate that the GA PID controller can suppress the vibration successfully. Moreover, the use of a proposed input shaper significantly reduced the vibrational displacement.

This experimental finding confirms that the GA PID with SS reduces vibrational displacement (RMS) without input shaping by approximately 41.25% at specific point 2 (Table 2) and by 45.49% at point 3 (Table 3). The controlled response confirms that the GA PID with SS can effectively suppress the vibration of the smart plate. Moreover, vibrational displacement can be further eliminated by as much as 43.18% for point 2 and 56.57% for point 3 when the ZVS is applied. Such control suppresses the transverse deflection of the structure. Thus, the proposed input shaping effectively reduces the vibrational displacement, especially when using the ZVS. These experimental results demonstrate the effectiveness of the proposed control methodology for minimizing vibrational displacement in the time domain. Similarly, the experiment also demonstrated that the GA PID with SS reduces the maximum amplitude around the resonant frequency caused by GA PID by approximately 45.68% (Table 2) and 29.38% (Table 3). The maximum amplitude can be further reduced, by as much as 64.42% (point 2) and 54.8% (point 3), when the ZVS is introduced. Thus, the proposed input shaping control scheme suppresses vibration amplitude not only in time domain, but also in frequency domain.

Table 2 Normalized RMS vibrational displacement subjected to the proposed control (point 2)

Control Type	**GA PD**	**GA PD+SS**	**GA PD+ZVS**
	(A)	**(B)**	**(C)**
Vib. Displacement (RMS)	0.02763	0.01623	0.01570
Vib. Displacement Reduction			
		(A-B)/A	(A-C)/A
(%)		**41.25%**	**43.18%**
Max. Displacement $\lvert Y(t)\rvert$	0.2119	0.1151	0.0754
Vib. Displacement Reduction %		(A-B)/A **45.68%**	(A-C)/A **64.42%**

Table 3 Normalized RMS vibrational displacement subjected to the proposed control (point 3)

Control Type	GA PD	GA PD+SS	GA PD+ZVS
	(A)	(B)	(C)
Vib. Displacement (RMS)	0.02436	0.01328	0.01058
Vib. Displacement Reduction (%)		(A-B)/A **45.49%**	(A-C)/A **56.57%**
Max. Amplitude $\lvert Y(t)\rvert$	0.1688	0.1192	0.0763
Max. Amplitude Reduction %		(A-B)/A **29.38%**	(A-C)/A **54.8%**

However, the PID controller tuned by the GA is capable of reducing the forced responses and thus can be operated in real time in an adaptive fashion. The experimental results of the actual process demonstrated that the proposed control method of combining PID tracking control and ZVS also suppresses the vibration effectively.

Consequently, combining input shaping with the feedback method yielded an improved performance for this system. A number of advantages of input shaping are evident, including: (1) it can eliminate motion-induced vibration resulting from modes that lie outside the bandwidth of a feedback controller, (2) shapers can be designed separately from the system motion, and (3) numerous methodologies have been developed to invent shapers that have a measure of robustness to system parameter uncertainties. Therefore, input shaping is a useful scheme for reducing vibration in large flexible structural systems.

5. Conclusions

A control scheme was developed to enable precise positioning of a MDOF structure system while eliminating motion-induced vibration. The control scheme utilized an architecture that allocates individual control objectives to the modules most suited for the task. A feedback control module based on genetic algorithm (GA) tuning was used to drive the plate to the desired position. Input shaping was used in another module to eliminate motion-induced vibrations. The positioning control module enabled the truss plate to achieve a desired position as well as reduce the motion-induced vibrations. As the tacking controller design was based on the approximated linear system, which includes some vibration, the dominant information came from the joint angle trajectory tracking. A more desirable input shaping control scheme allowed for elimination of these motion-induced vibrations in-depth. Experimental results verified that the proposed control methodology achieved excellent attenuated vibration due to the plate flexing. The effectiveness of vibration suppression was confirmed by applying the SS and ZVS. The investigation results also demonstrated that the PID with ZVS controller significantly outperformed the pure tracking PID-type controller. The broad range of problems discussed in this research is useful in civil, mechanical, and astronautical engineering for creating rotating flexible structures with MDOF

motion. Hence, the control of flexible robots, smart panels, tower cranes, aircraft fin-tip, satellites, and space stations that have solar array paddles are all the potential applications by using proposed control methodology to improve positioning and suppress motion-induced vibration.

Acknowledgements

The authors would like to thank the National Science Council of the Republic of China, Taiwan for financially supporting this research under Contract No. NSC 99-2221-E-231-023.

References

Blackburn, D., Lawrence, J., Danielson, J., Singhose, W., Kamoi, T. and Taura, A. (2010), "Radial motion assisted command shapers for nonlinear tower crane rotational slewing", *Control Eng. Pract.*, **18**(5), 523-531.

Chiang, C.B. (2012), *Vibration control for multi-degree-of-freedom flexible structural system*, Master Thesis, Chien Hsin University of Science and Technology.

Cutforth, C.F. and Pao, L.Y. (2003), "Control using equal length shaped commands to reduce vibration", *IEEE T. Control Syst. T.*, **11**(1), 62-72.

Cutforth, C.F. and Pao, L.Y. (2004), "Adaptive input shaping for maneuvering flexible structures", *Automatica*, **40**(4), 685-693.

Fujisaki, Y., Ikeda, M. and Miki, K. (2001), "Robust stabilization of large space structures via displacement feedback" *IEEE T. Automat. Contr.*, **46**(12), 1993-1996.

Hong, S., Park, H.C. and Park, C.H. (2006), "Vibration control of beam using multiobjective state-feedback control", *Smart Mater. Struct.*, **15**(1), 157-163.

Hu, Q. (2008), "Input shaping and variable structure control for simultaneous precision positioning and vibration reduction of flexible spacecraft with saturation compensation", *J. Sound Vib.*, **318**(1), 18-35.

Hyland, D.C., Junkins, J.L. and Longman, R.W. (1993), "Active control technology for large space structures", *J. Guid. Control Dynam.*, **16**(5)**,** 801-821.

Leissa, A.W. (1969) *Vibration of plates*, Scientific and Technical Information Division, National Aeronautics and Space Administration, Washington, D.C., USA.

Li, S., Qiu, J., Ji, H., Zhu, K. and Li, J. (2011), "Piezoelectric vibration control for all-clamped panel using DOB-based optimal control", *Mechatronics*, **21**(7), 1213-1221.

Lin, J. and Lewis, F.L. (2003), "Two-time scale fuzzy logic controller of flexible link robot arm", *Fuzzy Set. Syst.*, **139**(1)**,** 125-149.

Lin, J. (2005a), "An active vibration absorber of smart panel by using a decomposed parallel fuzzy control structure", *IFAC Eng. Appl. Artificial Intell.*, **18**(8) 985-998.

Lin, J. (2005b), "A vibration absorber of smart structures using adaptive networks in hierarchical fuzzy control", *J. Sound Vib.*, **287**(4-5), 683-705.

Lin, J. and Zheng, Y.B. (2012), "Vibration suppression control of smart piezoelectric rotating truss structure by parallel neuro-fuzzy control with genetic algorithm tuning *J. Sound Vib.*, **331**(16), 3677-3694.

Matsuno, F., Hatayama, M., Senda, H., Ishibe, T. and Sakawa, Y. (1996), "Modeling and control of a flexible solar array paddle as a clamped-free-free-free rectangular plate", *Automatica*, **32**(1), 49-58.

Moheimani, S., Vautier, B. and Bhikkaji, B. (2006), "Experimental implementation of extended multivariable PPF control on an active structure", *IEEE T. Control Syst. T.*, **14**(3), 443-455.

Nagashio, T. and Kida, T. (2009), "Robust control of flexible mechanical system by utilizing symmetry and its application to large space structures", *IEEE T. Control Syst. T.*, **17**(3), 671-680.

Park, J.Y. and Chang, P.H. (2001), "Learning input shaping technique for non-LTI systems", *Trans. ASME J.*

Dynam. Syst., Measure. Control, **123**(2), 288-293.
Qiu, Z.C., Zhang, X.M., Wu, H.X. and Zhang, H.H. (2007), "Optimal placement and active vibration control for piezoelectric smart flexible cantilever plate", *J. Sound Vib.*, **301**(3), 521-543.
Rao, A.K., Matesan, K., Bhat, M.S. and Ganguli, R. (2008), "Experimental demonstration of H_∞ control based active vibration suppression in composite fin-tip of aircraft using optimal placed piezoelectric patch actuators", *J. Intel. Mat. Syst. Str.*, **19**(6), 651-669.
Rhim, S. and Book, W.J. (2001), "Noise effect on adaptive command shaping methods for flexible manipulator control", *IEEE T. Control Syst. T.*, **9**(1), 84-92.
Singhose, W., Kim, D. and Kenison, M. (2008), "Input shaping control of double-pendulum bridge crane oscillation", *Trans. ASME J. Dynam. Syst., Measure. Control*, **130**(3), 0345041-0345047.
Sorensen, K.L., Singhose, W. and Dickerson, S. (2007), "A controller enabling precise positioning and sway reduction in bridge and gantry cranes", *Control Eng. Pract.*, **15**(7), 825-837.
Sorensen, K.L. and Singhose, W.E. (2008), "Command-induced vibration analysis using input shaping principles", *Automatica*, **44**(9), 2392-2397.
Tuttle, T.D. and Seering, W.P. (1996), "Vibration reduction in flexible space structures using input shaping on mace: mission results", *Proceedings of the IFAC World Congress (June)*, 55-60.
Vaughan, J., Yano, A. and Singhose, W. (2008), "Comparison of robust input shapers", *J. Vib. Sound*, **315**(4), 797-815.
Vaughan, J., Kim, D. and Singhose, W. (2010), "Control of tower cranes with double-pendulum payload dynamics", *IEEE T. Control Syst. T.*, **18**(6), 1345-1358.

CC